# Integrated Design of Navigation, Guidance and Control Systems for Unmanned Underwater Vehicles *

Daniel Fryxell, Paulo Oliveira, António Pascoal and Carlos Silvestre
Institute for Systems and Robotics and Department of Electrical Engineering
Instituto Superior Técnico
Av. Rovisco Pais, 1096 Lisboa Codex, Portugal

## Abstract

This paper describes an integrated approach to the design of navigation, guidance and control systems for Autonomous - Unmanned - Underwater Vehicles (AUVs). The framework adopted is illustrated with a design example in which recent developments in H-Infinity control theory, multi-rate navigation techniques and classical guidance strategies were applied to the design of a high level controller for the underwater vehicle MARIUS (Marine Utility Vehicle System). The problem statement requires the design of a command following system for the vehicle to achieve precise tracking of reference trajectories defined in an universal reference frame. This objective should be accomplished in the presence of shifting sea currents, sensor noise and vehicle parameter uncertainty. The design phase is described, and the interaction among navigation, control and guidance is analyzed. The performance of the complete command following system is evaluated using a simulation package that allows the designer to assess the impact of navigation, control and guidance algorithms on the dynamic performance of the vehicle.

## 1 Introduction

There is currently great interest in using Autonomous Underwater Vehicles (AUVs) to substantially reduce the costs and the risk associated with the exploration of the ocean. AUVs exhibit high maneuverability, and do note require permanent support from a ship or direct control via an umbilical cord. Furthermore, their operation does not jeopardize human lives directly. There are, however, concerns that the technologies required to achieve true autonomous behaviour are "necessarily advanced and remain developmental" [2]. The long term goal of using AUVs for the exploration of the ocean can only be achieved through a committed research and development effort aimed at developing sophisticated mobile units equipped with advanced systems for *navigation*, *guidance* and *control*.

This paper addresses the problem of designing guidance, navigation and control systems for AUVs to achieve accurate tracking of reference trajectories defined in an universal reference frame. See [10] for a comprehensive presentation of those systems, which are depicted in figure 1. The theoretical framework adopted is illustrated

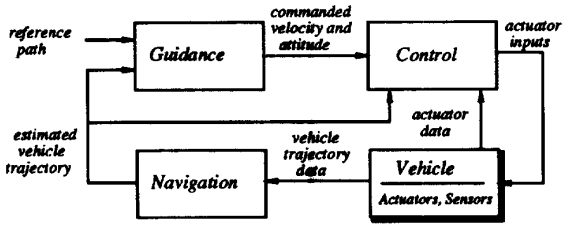


Figure 1: Navigation, Guidance and Control

with a design example in which recent developments in H-Infinity ( $\mathcal{H}_\infty$ ) control theory, multi-rate navigation techniques and classical guidance strategies, were applied to the design of a high level controller for the AUV MARIUS (Marine Utility Vehicle System) [4, 13]. The key ideas in the design methodology are to clearly state performance specifications in the frequency domain, and to use design tools that explicitly address these types of specifications. Thus, the natural constraint that the navigation, control and guidance systems have decreasing bandwidths, can be directly incorporated in the initial design phase. Analysis of the integrated system is performed using a simulation package that allows the user to assess the impact of the navigation, guidance, and control algorithms on the dynamic behaviour of the vehicle.

The organization of the paper reflects the natural sequence of steps in the design of a trajectory following system for an autonomous vehicle.

Section 2 introduces a dynamical model for the AUV MARIUS, based on hydrodynamic test data obtained at the Danish Maritime Institute in Lyngby, Denmark. Section 3 illustrates the design of a control system for the vehicle in the vertical plane. The selected method is

*This research work was supported in part by the Commission of the European Communities under contracts MAST-CT90-0059 and MAS2-CT92-0021 of the Marine Science and Technology Programmes (MAST-I and II), and in part by JNICT under contract PMCT/C/TIT/702/90. The tank tests at the Danish Maritime Institute were supported by the Technical University of Denmark and the Instituto Superior Técnico.



0-7803-2056-5 

$\mathcal{H}_\infty$ gain scheduled control, where the scheduling variable is dynamic pressure. Section 4 presents the basic motion sensor suite for MARIUS and provides a brief descriptiom of its multi-rate navigation system. Finally, Section 5 combines control and navigation with guidance. For a given reference trajectory, the performance of the vehicle is examined when the classical line-of-sight (LOS) guidance algorithm is used.

Due to space limitations, this paper presents only a brief survey of the work carried out. The reader is referred to [5, 6, 7] for complete details regarding the software package used for simulation and the design of the control, navigation and guidance systems.

# 2 Vehicle Modeling

This section introduces the dynamical model of the AUV MARIUS that is used for simulation and control systems design. The vehicle is depicted in figure 2. See [4, 13] for a complete description of the vehicle's design and construction. The general structure of the model

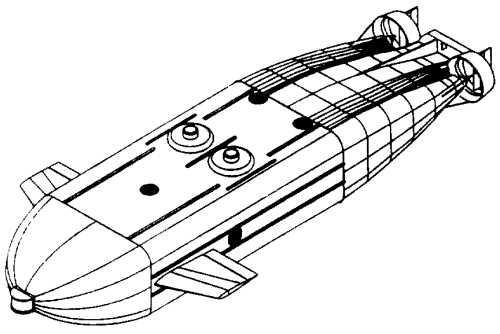

Figure 2: The vehicle MARIUS

is standard, and was simply derived from first physics principles, as explained in [1]. System identification, however, was far more complex and required the combination of theoretical and experimental methods that included tank tests with the full scale prototype of the vehicle. The tests are reported in [4, 12]. The estimated model can be found in [6], which contains a description of the methodologies used for modeling and identification.

## 2.1 Equations of Motion

The equations of motion for underwater vehicles can be obtained from Newton-Euler laws following the classical approach described by Abkowitz [1]. A simple and elegant derivation based on a general set-up adopted in robotics can be found in [14]. Using this approach, the equations are easily developed using a global coordinate frame $\{U\}$ and a body-fixed coordinate frame $\{B\}$ that moves with the AUV. This requires the following notation:

${}^U\mathbf{p}_{B_{org}} := (x, y, z)^T$ - position of the origin of $\{B\}$ measured in $\{U\}$,

${}^B\mathbf{v}_{B_{org}} := (u, v, w)^T$ - velocity of the origin of $\{B\}$ relative to $\{U\}$, expressed in $\{B\}$ (i.e., body-fixed linear velocity),

${}^B\omega_B := (p, q, r)^T$ - angular velocity of $\{B\}$ relative to $\{U\}$, expressed in $\{B\}$ (i.e., body-fixed angular velocity).

The symbol ${}^U_B R(\boldsymbol{\lambda})$ denotes the rotation matrix from $\{B\}$ to $\{U\}$, parameterized by the vector $\boldsymbol{\lambda} := (\phi, \theta, \psi)^T$ of roll, pitch and yaw angles. Let $\dot{\mathbf{q}} = (u, v, w, p, q, r)^T$ denote the vector of body-fixed linear and angular velocities, and let $\boldsymbol{\delta} := (\delta_{a,c}, \delta_{a,d}, \delta_e, \delta_r)^T$ be the vector whose entries are the deflections of the ailerons (common and differential), elevator, and rudder. Furthermore, let $n$ denote the rate of rotation of the main propellers. With this notation, the dynamics and kinematics of the AUV can be written in compact form as

Dynamics:

$$M_{RB}\ddot{\mathbf{q}} + C_{RB}(\dot{\mathbf{q}})\dot{\mathbf{q}} = \boldsymbol{\tau}(\ddot{\mathbf{q}}, \dot{\mathbf{q}}, \boldsymbol{\lambda}, \boldsymbol{\delta}, n), \tag{1}$$

$$\mathbf{q} = ({}^B\mathbf{v}^T_{B_{org}}, {}^B\omega^T_B)^T. \tag{2}$$

Kinematics:

$$\frac{d}{dt}({}^U\mathbf{p}_{B_{org}}) = {}^U_B R(\boldsymbol{\lambda})\,{}^B\mathbf{v}_{B_{org}}, \tag{3}$$

$$\frac{d}{dt}\boldsymbol{\lambda} = Q(\boldsymbol{\lambda})\,{}^B\boldsymbol{\omega}_B, \tag{4}$$

where $\boldsymbol{\tau}$ denotes the vector of external forces and moments that act on the vehicle and $Q(\boldsymbol{\lambda})$ is the matrix that relates body-fixed angular velocity with roll, pitch and yaw rates. The symbols $M_{RB}$ and $C_{RB}$ denote the rigid body inertia matrix and the matrix of Coriolis and centrifugal terms, respectively. The vector $\boldsymbol{\tau}$ can further be decomposed as

$$\begin{aligned}\boldsymbol{\tau}(\ddot{\mathbf{q}}, \dot{\mathbf{q}}, \boldsymbol{\lambda}, \boldsymbol{\delta}, n) &= \boldsymbol{\tau}_{rest}(\boldsymbol{\lambda}) \\ &+\boldsymbol{\tau}_{add}(\ddot{\mathbf{q}}, \dot{\mathbf{q}}) + \boldsymbol{\tau}_{lift}(\dot{\mathbf{q}}, \boldsymbol{\delta}) \\ &+\boldsymbol{\tau}_{visc}(\dot{\mathbf{q}}, \boldsymbol{\delta}) + \boldsymbol{\tau}_{prop}(n),\end{aligned} \tag{5}$$

where $\boldsymbol{\tau}_{rest}$ denotes the the forces and moments caused by gravity and buoyancy and $\boldsymbol{\tau}_{add}$ (added mass term) accounts for the dynamic forces and moments that would act on the vehicle assuming it were completely submerged in an inviscid fluid with no circulation. The term $\boldsymbol{\tau}_{lift}$ captures the effects of the lifting forces generated by the deflecting surfaces, $\boldsymbol{\tau}_{visc}$ consists of the forces and moments caused by skin friction and $\boldsymbol{\tau}_{prop}$ represents the forces and moments generated by the main propellers. The following notation will be used in the text: $\mathbf{V} = (u^2 + v^2 + w^2)^{1/2}$ denotes the absolute value of the velocity vector, $\alpha = arcsin(w/(u^2 + w^2)^{1/2})$ is the angle of attack and $\beta = arcsin(v/(u^2 + v^2 + w^2)^{1/2})$ is the angle of side-slip.

## 2.2 System Identification

To be of practical use, the model described by equations (1)-(4) must be tuned for the vehicle in study. Clearly, the main difficulty lies in computing the term $\tau$ that arises in the equation of dynamics. This was achieved by using both theoretical and experimental methods. The restoring term was easily computed from geometrical considerations, and the added mass term was computed by assuming ellipsoidal and elliptical cylinder approximations for the body and ailerons, respectively. Approximations for the lift term were obtained using thin airfoil theory. The viscous damping and propulsion terms were determined from the following series of tests carried out at the Danish Maritime Institute (DMI) in Lyngby, Denmark:

- Open water tests of the propeller/nozzle system to determine its characteristics in undisturbed (open) water,
- Resistance tests to measure the resistance of the vehicle without the propulsion system in place,
- Self-propulsion tests to assess the performance of the propulsion system in the wake of the hull,
- Planar Motion Mechanism tests in the horizontal and vertical planes to measure the most relevant hydrodynamic derivatives of the vehicle.

The methodology used for testing is reported in [4]. The most relevant test results can be found in [12]. See also [5, 6] for a description of the derived model used for simulation.

For control design purposes, the general model was divided into two sub-models for the horizontal and vertical planes. The sub-models do not include the kinematics equation (3), which is only relevant to the guidance system. In order to simplify the design phase, the vehicle was assumed to be commanded directly in thrust. Based on theoretical and experimental results available from tank tests, the simplified vertical model can then be formally written as

$$\frac{d}{dt}\mathbf{x}_v = \mathbf{f}_v(\mathbf{x}_v, \mathbf{u}_v), \tag{6}$$

where $\mathbf{x}_v = (u, w, q, \theta)^T \in \mathcal{R}^4$ is the state vector, $\mathbf{u}_v = (\delta_{a,c}, \delta_e, T)^T \in \mathcal{R}^3$ is the input vector and $\mathbf{f}_v : \mathcal{R}^4 \times \mathcal{R}^3 \rightarrow \mathcal{R}^4$ is a nonlinear function that is easily obtained from the surge, heave and pitch equations of motion [5, 6]. Identical procedure can be applied to the horizontal p...

# 3 Control System Design

This section focuses on the design of a control system for the AUV MARIUS. The methodology adopted is gain-scheduled control, whereby the design of a controller to achieve stabilization and adequate performance of a given nonlinear plant follows four basic steps:

i) Linearizing the plant about a finite number of representative operating points,

ii) Designing linear controllers for the plant linearizations at each operating point,

iii) Interpolating the parameters of the linear controllers of Step ii) to achieve adequate performance of the linearized closed-loop systems at all points where the plant is expected to operate. The interpolation is performed according to an external scheduling vector (e.g., dynamic pressure and angle of attack), and the resulting family of linear controllers is referred to as *gain scheduled controller*,

iv) Implementing the gain scheduled controller on the original nonlinear plant.

## 3.1 System Linearization. Control design requirements

The model for the vertical plane was rewritten in terms of the angle of attack $\alpha$ and total velocity $\mathbf{V}$, and linearized about the equilibrium point determined by $\mathbf{x}_{v_0}=(\mathbf{V}_0, \alpha_0, q_0, \theta_0)^T = (1.26\ m/s, 0, 0, 0)^T$ and $\mathbf{u}_{v_0} = (\delta_{a,c_0}, \delta_{e_0}, T_0)^T=(0, 0, 77.2N)^T$ to obtain the linear system $\mathcal{P}$ with realization $\{A, B, C\}$, where $A = A(\mathbf{x}_{v_0}, \mathbf{u}_{v_0}) = \frac{\partial}{\partial \mathbf{x}_v}\mathbf{f}(\mathbf{x}_{v_0}, \mathbf{u}_{v_0}), B = B(\mathbf{x}_{v_0}, \mathbf{u}_{v_0}) = \frac{\partial}{\partial \mathbf{u}_v}\mathbf{f}(\mathbf{x}_{v_0}, \mathbf{u}_{v_0})$ and $C = I$.The linear controller for the linearized plant model $\mathcal{P}$ was required to satisfy the following design requirements:

1. **Zero Steady State Error.** Achieve zero steady state values for all error variables in response to command inputs in pitch ($\theta_{cmd}$), angle of attack ($\alpha_{cmd}$) and forward velocity ($\mathbf{V}_{cmd}$).
2. **Bandwidth Requirements.** The input-output command response bandwidth for all command channels should be on the order of 0.1 $rad/s$; the control loop bandwidth for all actuators should not exceed 0.5 $rad/s$ (these figures were selected to ensure that the actuators were not be driven beyond their normal bandwidth).
3. **Closed Loop Damping and Stability Margins.** The closed loop eigenvalues should have a damping ratio of a least 0.6. Classical gain and phase margins of 6 $db$ and 45 $deg$ should be satisfied in all control loops (one loop at a time analysis).

## 3.2 Linear Control System Design: The $\mathcal{H}_\infty$ Synthesis Approach

The methodology selected for linear control system design was $\mathcal{H}_\infty$ theory. This design method rests on a firm theoretical basis, and leads naturally to an interpretation of control design specifications in the frequency domain. Furthermore, it provides clear guidelines for the design of controllers so as to achieve robust performance in the presence of plant uncertainty. See [3] for an elegant

solution to the problem of $\mathcal{H}_\infty$ control design using a state-space framework and [9] for a case study.

In what follows, we adopt the general set-up and nomenclature in [3]. This leads to the standard feedback system of figure 3, where $\mathcal{P}$ is the linearized model of the AUV in the vertical plane and $\mathcal{K}$ is the controller to be designed. The symbol **w** denotes the input vector of exogenous signals, **z** is the output vector of errors to be reduced, **y** is the vector of measurements that are available for feedback and **u** is the vector of actuator signals. The generalized plant $\mathcal{G}$ consists of the physical plant to be controlled, together with appended weights that shape the exogenous and internal signals. In practice, the weights serve as tuning "knobs" which the designer can adjust to meet the desired performance specifications. Suppose that the feedback system is well-posed, and let

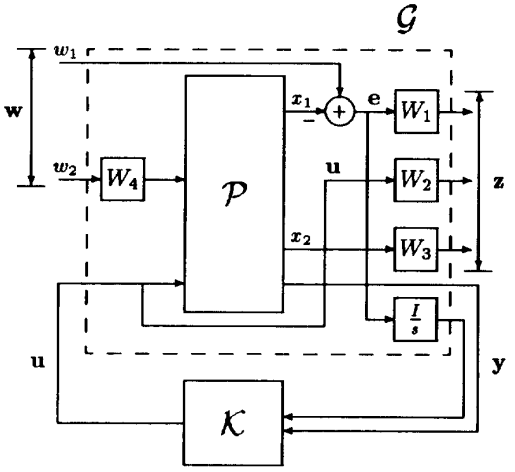


Figure 3: Synthesis model.

$\mathcal{T}_{\mathbf{zw}}$ denote the closed loop transfer matrix from **w** to **z**. The $\mathcal{H}_\infty$ synthesis problem consists of finding, among all controllers that yield a stable closed loop system, a controller $K$ that minimizes the infinity norm $\|\mathcal{T}_{\mathbf{zw}}\|_\infty$ of the operator $\mathcal{T}_{\mathbf{zw}}$. We remind the reader that $\|\mathcal{T}_{\mathbf{zw}}\|_\infty$ equals $\sup\{\sigma_{\max}(\mathcal{T}_{\mathbf{zw}}(j\omega)) : \omega \in \Re\}$, where $\sigma_{max}(.)$ denotes the maximum singular value of a matrix. The norm $\|\mathcal{T}_{\mathbf{zw}}\|_\infty$ may be interpreted as the maximum energy gain of the closed loop operator $\mathcal{T}_{\mathbf{zw}}$. In practice, it is not necessary to find the exact optimal $\mathcal{H}_\infty$ controller. In fact, suboptimal controllers with performances arbitrarily close to the optimal one can be easily generated using numerically robust algorithms, see for example [9] and the references therein.

The following signals and weights were used in the design of a controller for the vertical plane: the signal $w_1$ represents the vector of input commands which must be tracked - it consists of velocity, angle of attack and pitch commands, denoted $\mathbf{V}_{cmd}$, $\alpha_{cmd}$ and $\theta_{cmd}$, respectively. The signal $w_2$ represents the noise inputs to each of the measured variables, and the disturbance inputs to the states of the plant. The signal **u** represents the control inputs to the system - it consists of the actuator signals for common aileron deflection $\delta_{a,c}$, elevator deflection $\delta_e$ and thruster command $T$. The signal $x_1$ represents the components of the state vector that must track the input commands and consists of **V**, $\alpha$ and $\theta$. The vector $\mathbf{e} = w_1 - x_1 = (V_e, \theta_e, \alpha_e)^T$ contains the respective tracking errors. The signal $x_2$ contains the remaining state variable - pitch rate $q$ - that must be weighted.

The outputs of $W_1$, $W_2$, and $W_3$ constitute the vector **z** of errors to be reduced. Since zero steady-state errors in tracking the step command for all variables in $x_1$ was required, the weighting function $W_1$ was chosen as $W_1$=diag $(\frac{2}{s}, \frac{1}{s}, \frac{1}{s})$, where the integrator gains have been adjusted to get the desired command response bandwidths. The weights $W_2 = diag(1, 1, 0.1)$ and $W_3 = 1$ were selected to meet the additional desired specifications. The signal **y** includes all the states of the plant $\mathcal{P}$, together with the appended states that correspond to the integrators, that is, $\mathbf{y}=(\mathbf{V}, \alpha, q, \theta, \frac{V_e}{s}, \frac{\alpha_e}{s}, \frac{\theta_e}{s})$.

### 3.3 Non-linear Controller Implementation

A set of controllers was determined for three values of forward speed following the methodology exposed in section 3, and their parameters interpolated according to the scheduling variable **V**, see [6]. The implementation of the resulting non-linear gain scheduled controller was done using the $D$-methodology described in [8]. This approach guarantees the following fundamental *linearization property*: at each equilibrium point, the linearization of the nonlinear feedback control system preserves the internal as well as the input-output properties of the corresponding linear closed loop designs. This property is often not satisfied in gain scheduled controllers proposed in the literature, see [8] and the references therein. In practice, violation of that property may lead to degradation in performance, or even instability, of the closed -loop system. It is interesting to remark that the $D$-methodology leads naturally to gain scheduled controllers with integrators directly at the input of the plant. This fact makes the implementation of anti-windup schemes straightforward [7]. In the work reported here, the gain scheduled controller was discretized at a sampling rate of $10Hz$.

## 4 Navigation System Design

This section describes the basic framework used in the design of the navigation system for the AUV MARIUS. The objective is to obtain accurate estimates of the position and attitude of the vehicle, based on measurements available from a motion sensor package installed on-board. The estimates are input to the controller derived in section 3, and to the guidance system of section 5.

In this paper we adopt a conceptually simple framework for filtering that is rooted in the kinematic relationships expressed by equations (3) and (4). This approach

borrows from the theory of *complementary filtering* exposed in [10], see [5] for complete details. The approach leads naturally to the design of linear, time-invariant Kalman filters, whereby the covariance of the process and observation noises are viewed as tuning knobs to shape the frequency responses from measured to estimated variables. This methodology bears great affinity with the general procedure for control system design explained in section 3.

### 4.1 Attitude Estimation

The motion sensor package of MARIUS includes two *pendulums* that provide - indirectly - measurements $\phi_m$ and $\theta_m$ of roll and pitch angles, respectively, one *gyrocompass* that provides measurements ($\psi_m$) of yaw angle, and three *rate gyroscopes* whose outputs $p_m, q_m, r_m$ correspond to the angular body rates $p, q, r$. Let $\Lambda_m = (\phi_m, \theta_m, \psi_m)$ and ${}^B\omega_{B_m} = (p_m, q_m, r_m)$. For a sampling time of $h$ seconds, the discrete-time complementary filter that provides corrected estimates of roll, pitch and yaw angles and angular body rates based on the information available from the sensors described, is given by

$$\begin{aligned}
\mathbf{x}_1(k+1) &= \mathbf{x}_1(k) + h[\mathbf{x}_2(k) + Q(\mathbf{x}_1(k)){}^B\omega_{B_m}(k)] \\
&\quad + K_1(\Lambda_m(k) - \mathbf{x}_1(k)) \\
\mathbf{x}_2(k+1) &= \mathbf{x}_2(k) + K_2(\Lambda_m(k) - \mathbf{x}_1(k)) \\
\hat{\Lambda}(k) &= \mathbf{x}_1(k) \\
{}^B\hat{\omega}_B(k) &= {}^B\omega_{B_m}(k) + Q(\mathbf{x}_1(k))^{-1}\mathbf{x}_2(k),
\end{aligned}$$

where $\hat{\Lambda}$ and ${}^B\hat{\omega}_B$ denote the estimates of $\Lambda$ and ${}^B\omega_B$ respectively, $K_1 \in \mathcal{R}^{3\times3}$ and $K_2 \in \mathcal{R}^{3\times3}$ are filter Kalman gains and $Q(.)$ is the matrix in (4). The filter provides natural rejection of constant rate gyro bias terms. In the design example reported here, the Kalman gains were selected so that the filter bandwiths corresponding to the transfer functions from each angle and angle rate measurement to the corresponding estimates would be on the order of $15 rad/s$ (that is, much larger than the bandwidths of the corresponding control loops). The sampling interval adopted was $h = 0.01s$.

### 4.2 Linear Position and Velocity Estimation

The following sensor units are used to provide measurements of the linear position and velocity of the vehicle: a *long baseline positioning system* (LBL) that computes the roundtrip travel times of acoustic pulses that are emitted by the vehicle and returned by an array of transponders (a triangulation algorithm is used to provide measurements of ${}^U\mathbf{p}_{B_{org}} := (x, y, z)^T$), a *depth cell* that provides direct measurements of depth coordinate $z$, and a Doppler sonar that measures the body fixed velocity vector ${}^B\mathbf{v}_{B_{org}} := (u, v, w)^T$. A simple *paddle wheel* sensor is used as a back-up instrument to provide measurements of $u_w$, where the subscript denotes that the velocity is computed with respect to the water.

An integrated filter to provide corrected estimates of position and velocity of the vehicle with respect to the seabed can now be designed following an approach similar to that described in section 4.1. Notice, however, that due to the characteristics of the acoustic channel, the measurements from the LBL system are available at a rate that is much smaller than that of the remaining sensors. This problem can be tackled using multi-rate Kalman filter theory exposed in [11, 15]. See [5] for the design of a multi-rate filter for the vehicle, where the sampling rate of the LBL system and that of the other sensors are $0.2\,Hz$ and $1\,Hz$, respectively.

## 5 Guidance. Integrated Simulation with Navigation and Control.

The purpose of the guidance system is to generate the references that are applied to the AUV's control system in order to achieve accurate tracking of paths specified in an universal reference frame $\{U\}$. Conceptually, the design of the guidance system is rather simple as it relies solely on the kinematics equation (3) of Section 2. The reader is referred to [6] for complete details regarding the line-of-sight guidance law used in this study. The combined performance of the guidance, navigation

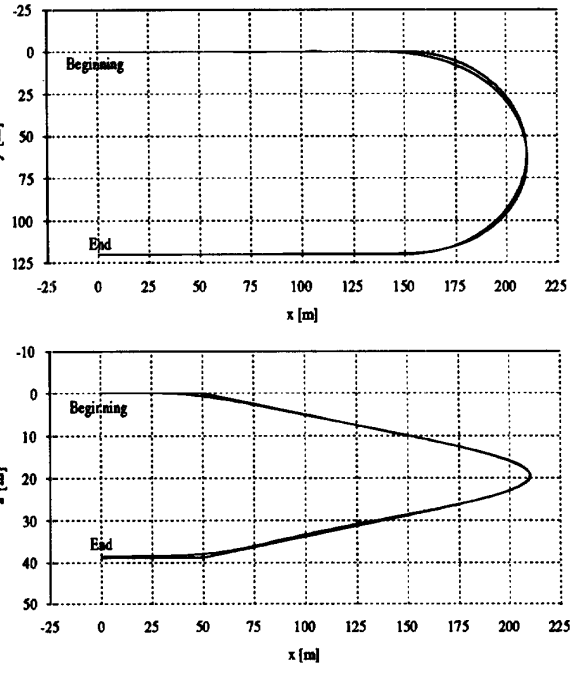


Figure 4: Reference and observed trajectory - horizontal and vertical planes.

and control systems was evaluated in simulation with the nonlinear model of the vehicle. The simulation included physically based models of the sensor units described in section 4, as well as the dynamics of the thrusters and their control systems. In order to simplify the interpretation of the simulation results, the velocity command $\mathbf{V}_c$ was held constant at $1.26m/s$. The references to roll and angle of attack were set to zero.

The reference for linear position is an $\mathcal{U}$ - shaped trajectory that descends smoothly along the depth coordinate $z$. Its projection on the horizontal plane consists of two straight lines joined by a semi-circumference with 60 $m$ radius. The projection on the vertical plane consists roughly of two horizontal lines joined by two straight lines with a slope of $-10$ deg. Throughout the trajectory, the vehicle is subject to a uniform current with velocity $V_w = (0, 0.5m/s., 0)$ along the inertial $y$ coordinate. The desired and observed trajectories are depicted in figure 4. The evolution of the control inputs and the activity of some relevant state variables are condensed in figures 5 and 6. In this simulation, the LBL system uses four transponders located in positions $\{-40, 0, 160\}, \{130, 0, 150\}, \{-40, 90, 170\}$ and $\{140, 90, 135\}$.

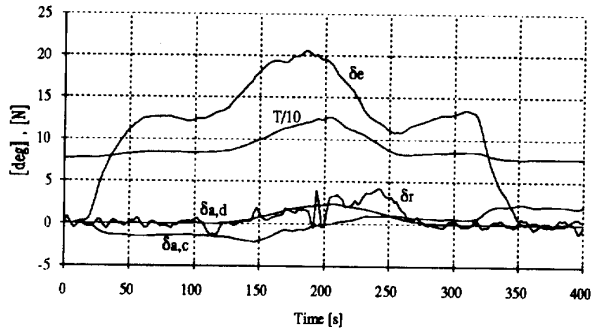


Figure 5: Control activity: Rudder ($\delta_r$), Ailerons ($\delta_{a,c}$ and $\delta_{a,d}$), Elevator ($\delta_e$) and Thruster ($T$).

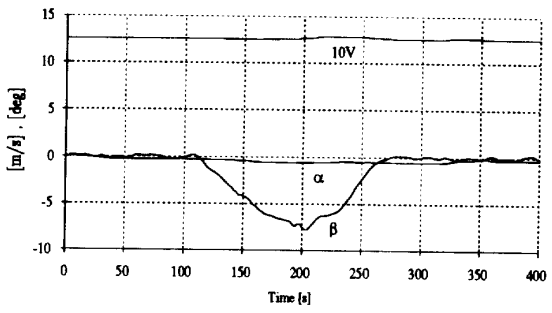


Figure 6: Velocity ($\mathbf{V}$), sideslip angle ($\beta$) and angle of attack ($\alpha$).

# References


[1] M. Abkowitz, "Lectures on Ship Hydrodynamics - Steering and Maneuverability," *report No. Hy-5, Hydrodynamics Department*, Technical University of Denmark, Lyngby, Denmark, May 1964.

[2] J. Bellingham, "Capabilities of Autonomous Underwater Vehicles," *Proceedings of the Workshop on Scientific and Environmental Data Collection with Autonomous Underwater Vehicles*, Cambridge,Massachusetts, US, March 1992, pp. 7-14.

[3] J. C. Doyle, K. Glover, P. P. Khargonekar, and B. A. Francis, "State space solutions to standard $\mathcal{H}_2$ and $\mathcal{H}_\infty$ control problems," *IEEE Transactions on Automatic Control*, AC- 34(8), August 1989,pp. 831-847.

[4] P. Egeskov, A. Bjerrum, A. Pascoal, C. Silvestre, C. Aage and L. Wagner Smitt,"Design, Construction and Hydrodynamic Testing of the AUV MARIUS," *Proc. AUV 94*, Cambridge, Massachusetts, 1994.

[5] D. Fryxell, P. Oliveira, A. Pascoal and C. Silvestre "Modeling, Identification and Control of the AUV MARIUS," *SOUV-Technical Report*, Institute for Systems and Robotics, March 1994.

[6] D. Fryxell, *Modeling, Identification, Guidance and Control of an Autonomous Underwater Vehicle*, MSc Thesis, Department of Electrical Engineering, Instituto Superior Técnico, March 1994.

[7] D. Fryxell, P. Oliveira, A. Pascoal and C. Silvestre "An Integrated Approach to the Design and Analysis of Navigation, Guidance and Control Systems for AUVs," *Proceedings of the Symposium on Autonomous Underwater Vehicle Technology,*, Cambridge, Massachusetts, July 1994.

[8] I. Kaminer, A. M. Pascoal, P. P. Khargonekar, and C. Thomson,"A velocity algorithm for the implementation of gain-scheduled nonlinear controllers," *Proceedings of the second European Control Conference*, June 1993, pp. 787-792.

[9] I. Kaminer, A. M. Pascoal, C. Silvestre, and P. P. Khargonekar, "Design of a control system for an underwater vehicle using $\mathcal{H}_\infty$ synthesis," *Proceedings of the 30th Conference on Decision and Control*,December 1991.

[10] C. Lin, *Modern Navigation, Guidance, and Control Processing*, Prentice-Hall, 1991.

[11] R. Meyer, and S. Burrus, "A unified analysis of multirate and periodically time-varying digital filters," *IEEE Transactions on Circuits and Systems*, CAS-22(3), March 1975, pp. 162-168.

[12] Axel Mølgaard, "PMM Tests with the Autonomous Underwater Vehicle MARIUS," *Technical Report No.1*, DMI 1152.92167, Danish Maritime Institute, March 1993.

[13] A. Pascoal,"The AUV MARIUS: mission scenarios, vehicle design, construction and testing," *Proceedings of the 2nd Workshopon Mobile Robots for Subsea Environments*, Monterey Bay Aquarium, Monterey, California USA, May 1994.

[14] C. Silvestre, *Modeling and Control of Autonomous Underwater Vehicles*, MSc Thesis, Instituto Superior Técnico, Lisbon, 1991.

[15] C. de Souza, "Periodic strong solution for the optimal filtering problem of linear discrete-time periodic systems," *IEEE Transactions on Automatic Control*, AC-36(3), March 1991, pp. 333-337.